RAGE signaling sustains inflammation and promotes tumor development

Christoffer Gebhardt,[1,4] Astrid Riehl,[1] Moritz Durchdewald,[1] Julia Németh,[1] Gerhard Fürstenberger,[2] Karin Müller-Decker,[2] Alexander Enk,[4] Bernd Arnold,[3] Angelika Bierhaus,[5] Peter P. Nawroth,[5] Jochen Hess,[1] and Peter Angel[1]

[1]Division of Signal Transduction and Growth Control, [2]Research Group Eicosanoids and Tumor Development, and [3]Division of Molecular Immunology, German Cancer Research Center, 69120 Heidelberg, Germany
[4]Department of Dermatology, University Hospital Heidelberg, 69115 Heidelberg, Germany
[5]Department of Medicine I and Clinical Chemistry, University Hospital Heidelberg, 69120 Heidelberg, Germany

A broad range of experimental and clinical evidence has highlighted the central role of chronic inflammation in promoting tumor development. However, the molecular mechanisms converting a transient inflammatory tissue reaction into a tumor-promoting microenvironment remain largely elusive. We show that mice deficient for the receptor for advanced glycation end-products (RAGE) are resistant to DMBA/TPA-induced skin carcinogenesis and exhibit a severe defect in sustaining inflammation during the promotion phase. Accordingly, RAGE is required for TPA-induced up-regulation of proinflammatory mediators, maintenance of immune cell infiltration, and epidermal hyperplasia. RAGE-dependent up-regulation of its potential ligands S100a8 and S100a9 supports the existence of an S100/RAGE-driven feed-forward loop in chronic inflammation and tumor promotion. Finally, bone marrow chimera experiments revealed that RAGE expression on immune cells, but not keratinocytes or endothelial cells, is essential for TPA-induced dermal infiltration and epidermal hyperplasia. We show that RAGE signaling drives the strength and maintenance of an inflammatory reaction during tumor promotion and provide direct genetic evidence for a novel role for RAGE in linking chronic inflammation and cancer.

CORRESPONDENCE
Peter Angel:
p.angel@dkfz.de

Human cancer develops via a multistep process that can be divided both operationally and mechanistically into three phases: initiation, promotion, and progression (1, 2). Several lines of evidence, including general or tissue-specific gene inactivation in mice and population-based studies, support the assumption that inflammation plays an important role during carcinogenesis (3, 4). Therefore, it is widely accepted that many neoplastic diseases are driven, at least in part, by chronic and often subclinical inflammation (4, 5). Chemically induced skin carcinogenesis is one of the best-established in vivo models to study the multistage nature of tumor development, and it represents a classical inflammation-associated tumor model, as its promotion phase solely depends on repeated topical treatments with TPA, a potent inducer of dermal inflammation (2, 6). Moreover, antiinflammatory treatment during the promotion phase with dexamethasone or nonsteroidal antiinflammatory drugs interferes with TPA-induced tumor formation (4). Despite this experimental evidence, the exact molecular mechanisms linking sustained, "smoldering" inflammation and carcinogenesis in this chemically induced tumor model still remain largely elusive. Recent data have highlighted the importance of proinflammatory signaling pathways in tumor promotion, because mice deficient for the cytokine *Tnf*-α or its receptors (*Tnfr1* or *2*) are resistant to DMBA/TPA-induced skin carcinogenesis (4, 7).

In this report, we describe a novel mechanistic role for the receptor for advanced glycation end-products (RAGE) in linking inflammation and cancer using a defined genetic *Rage* knockout mouse model. RAGE is a member of the immunoglobulin superfamily that has multiple extracellular ligands, is implicated in the pathogenesis of various inflammatory disorders, and plays a potent role in innate immunity (8, 9). *Rage*-deficient mice are protected from the lethal effects of septic shock caused by cecal ligation

P. Angel and J. Hess contributed equally to this work.
The online version of this article contains supplemental material.

The Journal of Experimental Medicine

Downloaded from http://rupress.org/jem/article-pdf/205/2/275/1897784/jem_20070679.pdf by guest on 09 February 2026

and puncture (10), providing experimental evidence for its contribution, at least in part, to the development of distinct inflammatory diseases (8, 9). In the context of cancer, elevated expression levels of RAGE and its ligands have been detected in a growing number of tumor types (8, 11). We demonstrate that RAGE signaling drives tumor development by sustaining inflammation during the promotion phase of chemically induced carcinogenesis, and define key proinflammatory mediators and cytokines as novel targets of RAGE signaling. Given the close association between chronic inflammation and epithelial cancer, we propose that RAGE activation by its ligands establishes a sustained tissue activation, which over time promotes tumor development.

RESULTS AND DISCUSSION

To elucidate the role of RAGE in multistage skin carcinogenesis, we subjected wild-type (*wt*) and *Rage*-deficient ($Rage^{-/-}$) female mice to a single topical application with the carcinogen DMBA, followed by promotion with the phorbol ester TPA for 30 wk. After 8 wk of promotion, tumors were exclusively found on *wt* back skin, and by 13 wk all *wt* mice had developed tumors (Fig. 1 A, left). In contrast, $Rage^{-/-}$ mice developed the first tumors after 14 wk of promotion ($P < 0.0001$ for the time to first tumor appearance), and the maximal tumor incidence was only 58%. Moreover, we detected a highly significant difference ($P < 0.0001$) in tumor multiplicity, with 5.1 tumors per mouse in *wt* controls but only 1.1 tumors per mouse in $Rage^{-/-}$ animals (Fig. 1 A, right). Overall, $Rage^{-/-}$ tumors were smaller in size, appeared less progressed, and were highly differentiated and hyperkeratotic (Fig. 1 B; and Fig. S1, available at http://www.jem.org/cgi/content/full/jem.20070679/DC1). Detailed analysis of tissue sections derived from $Rage^{-/-}$ tumors in comparison to *wt* tumors by immunohistochemistry (IHC) revealed a significantly lower level of Ki67- and BrdU-positive tumor cells ($P < 0.0001$; Fig. 1 C and Fig. S2 A), as well as fewer cells showing Jun protein phosphorylation (Fig. S2 B), a protooncogenic transcription factor of the activator protein 1 family crucial for keratinocyte proliferation and neoplastic transformation (12, 13). We also found increased apoptosis of epidermal tumor cells in $Rage^{-/-}$ tumors compared with *wt* controls using a Tdt-mediated dUTP-biotin nick-end labeling (TUNEL) assay (Fig. 1 D) in concert with a significant decrease ($P < 0.0001$) in nuclear staining for phosphorylated p65/RelA, a member of the NF-κB transcription factor implicated in antiapoptotic signaling (14), using indirect immunofluorescent (IF) analysis (Fig. 1, D and E). Thus, the reduction in tumor size of $Rage^{-/-}$ mice may be at least partially explained by the low proliferation rate and the increase in apoptosis.

Importantly, histological analysis of *Rage*-deficient tumors revealed significantly impaired stromal infiltration by mast cells ($P < 0.0001$), macrophages ($P < 0.0001$), and neutrophils ($P < 0.003$) compared with *wt* controls (Fig. 2 A and Fig. S2 C), suggesting RAGE-dependent activation of an inflammatory tumor microenvironment. Extended analysis further indicated that *wt* tumors harbor myeloid cells of the $CD11b^+$ $Gr\text{-}1^+$ subset that were not found in $Rage^{-/-}$ tumors (Fig. S2 D). These cells are known to induce T lymphocyte dysfunction and, therefore, actively inhibit antitumor adaptive immunity (5).

As a potent activator of inflammation, TPA triggers strong up-regulation of proinflammatory mediators and cytokines that subsequently results in dermal infiltration by immune cells and in epidermal hyperplasia (2). To test whether *Rage* deficiency affects the kinetics and dynamics of the transient inflammatory response induced by TPA, we studied the dermal infiltration in *wt* and $Rage^{-/-}$ back skin over time. 6 h after a single TPA application in *wt* skin, dermal infiltration by neutrophils, macrophages, and mast cells was observed by histological examination, and by specific IF analysis with a further increase after 12 h (Fig. 2, B and C). Strong dermal infiltration was maintained for 24 h but decreased 48 h after TPA application. Although an initial dermal infiltration was also seen in $Rage^{-/-}$ skin sections after 6 and 12 h, significantly fewer innate immune cells were detected compared with *wt* controls at 24 and 48 h (mast cells, $P < 0.001$; macrophages, $P < 0.001$; neutrophils, $P < 0.001$; Fig. 2, B and C). Similar data were also obtained with DMBA-pretreated animals (Fig. S3, available at http://www.jem.org/cgi/content/full/jem.20070679/DC1), excluding a major impact of DMBA initiation on the proinflammatory response of TPA on mouse back skin.

Our observation that ablation of RAGE signaling causes impaired tumor growth is consistent with previous data by Taguchi et al., who observed suppression of TPA-induced tumor formation in a *v-Ha-ras*–transgenic mouse tumor model using sRAGE, a soluble antagonist of RAGE (15). However, in this study both the effect of sRAGE treatment on the inflammatory response and the functional mechanism for RAGE signaling during tumor promotion remained undefined. Moreover, it is important to note that sRAGE has an impact on multiple immune responses even in the absence of functional RAGE, leading to the assumption that the beneficial effects of sRAGE in mouse disease models are not solely caused by preventing ligand engagement of RAGE (10).

To identify functional candidate genes that reflect the differences in the transient TPA response between *wt* and $Rage^{-/-}$ skin, we analyzed the expression kinetics of proinflammatory genes that are known to be important players in skin carcinogenesis (7, 16). Real-time quantitative PCR (RQ-PCR) with complementary DNA (cDNA) samples of skin derived from distinct time points after a single TPA treatment revealed an impaired induction of *Prostaglandin-endoperoxide synthase 2* (*Ptgs2*) in $Rage^{-/-}$ skin samples compared with *wt* controls (Fig. 3 A). *Ptgs2* encodes for the proinflammatory mediator cyclooxygenase-2 (COX-2), and indirect IF analysis on DMBA/TPA-induced tumor sections with a COX-2–specific antibody revealed only scarce positive staining in $Rage^{-/-}$ samples, whereas strong staining was detected in both tumor and stromal cells of *wt* controls (Fig. S4, available at http://www.jem.org/cgi/content/full/jem.20070679/DC1). These data are in accordance with recent findings demonstrating a RAGE-dependent *Ptgs2* up-regulation in distinct cell types (17, 18), and

Downloaded from http://rupress.org/jem/article-pdf/205/2/275/1897784/jem_20070679.pdf by guest on 09 February 2026

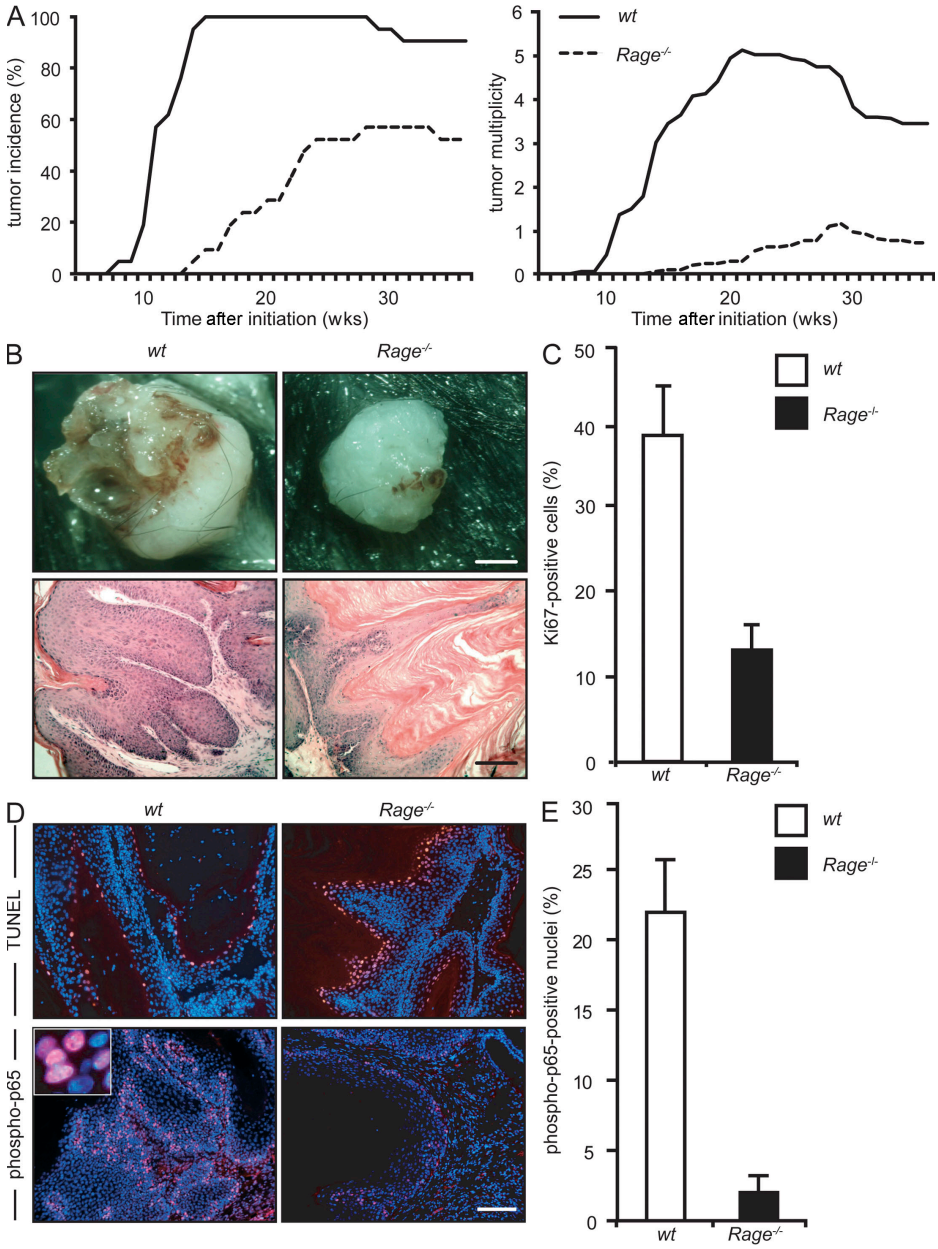

Figure 1. *Rage*$^{-/-}$ mice are protected against DMBA/TPA-induced tumor development. (A) *wt* and *Rage*$^{-/-}$ mice were subjected to the DMBA/TPA skin carcinogenesis protocol and were assessed and statistically analyzed as described in Materials and methods. The graphs display the number of tumor-bearing mice (left, incidence) and the mean number of tumors per mouse (right, multiplicity) at the indicated time points after DMBA treatment. (B) Representative macroscopic pictures (top) and bright-field microscopic views of hematoxylin-eosin–stained sections (bottom) of *wt* and *Rage*$^{-/-}$ tumors. Bars: (top) 1 mm; (bottom) 200 µm. (C) The percent total of Ki67-labeled tumor cells of three tumors from each genotype was calculated as described in Materials and methods. (D) Representative pictures of *wt* and *Rage*$^{-/-}$ tumor sections that were analyzed by TUNEL assay (top, red signal) and by indirect IF staining of phospho-p65 protein (bottom, red signal), as described in Materials and methods. Nuclear staining was done with H33342 (blue signal). Inset shows a higher magnification of phospho-p65 stained nuclei. Bar, 100 µm. (E) The percent total of phospho-p65–labeled tumor cells within three tumors from each genotype was calculated as described in Materials and methods. Error bars represent the SEM.

regarding the important role of this enzyme as a proinflammatory mediator representing a major target for cancer chemoprevention by nonsteroidal antiinflammatory drugs (16, 19). Indeed, ectopic COX-2 overexpression in the skin of transgenic mice is sufficient to transform the epidermis into an "autopromoted" state and to drive tumor development in DMBA-initiated skin without TPA treatment (19).

In TPA-treated *wt* skin, we also measured dramatic changes for the macrophage inflammatory protein (MIP) family members *Mip-1α*, *Mip-1β*, and *Mip-2* using RQ-PCR, whereas

Downloaded from http://rupress.org/jem/article-pdf/205/2/275/1897784/jem_20070679.pdf by guest on 09 February 2026

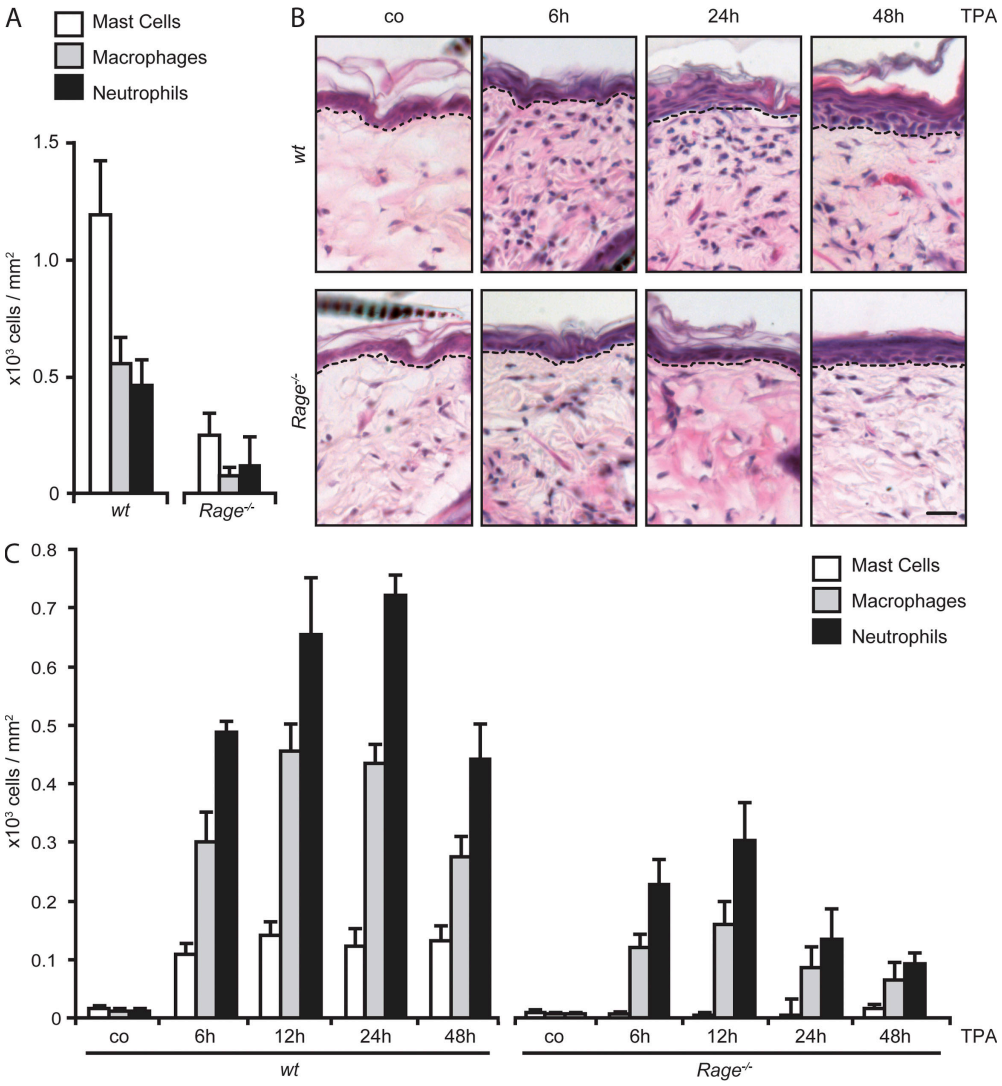

Figure 2. Impaired inflammatory response in *Rage*$^{-/-}$ mice. (A) Innate immune cells within the stroma of at least six *wt* and *Rage*$^{-/-}$ tumors were counted based on indirect IF stainings for neutrophils (antineutrophils, black bars) and macrophages (anti-CD68, gray bars), or on toluidine blue staining for mast cells (white bars), and are given as cells per square millimeter. Values represent means ± SEM from three mice from each genotype. (B) Representative pictures of hematoxylin-eosin–stained *wt* and *Rage*$^{-/-}$ skin specimens that were collected at the indicated time points after a single topical treatment of acetone (co) or 10 nmol TPA in acetone. Dashed lines indicate the border between the epidermis and dermis. Bar, 20 µm. (C) Innate immune cells within the dermis of at least three *wt* and *Rage*$^{-/-}$ mice treated as described in B were counted based on specific stainings and analyzed as described in A.

mild differences in *Tnf-α* induction and only minor alterations for *Tgf-β* transcript levels were observed (Fig. 3 A). In contrast, only marginal induction was seen in *Rage*$^{-/-}$ skin, demonstrating that these well-known effectors of chemotaxis and inflammation are novel targets of RAGE signaling. IHC analysis confirmed reduced amounts of infiltrating immune cells and/or epithelial cells expressing MIP proteins in back skin upon a single TPA application or within *Rage*$^{-/-}$ tumors (Fig. 3 B; and Figs. S4 and S5, available at http://www.jem.org/cgi/content/full/jem.20070679/DC1). MIP-1α, MIP-1β, and MIP-2 are chemokines responsible for the recruitment of polymorphonuclear cells at sites of inflammation (20), and mice deficient for their scavenging decoy receptor D6 were characterized by an excess concentration of residual chemokines, a sustained inflammatory response to TPA (20), and an increased susceptibility to tumor development in the DMBA/TPA model (21).

The targets of RAGE signaling identified in the present study are well-known target genes of NF-κB, an essential player in the neoplastic transformation of keratinocytes and in linking inflammation to cancer development and progression (14, 22). In this context, it is noteworthy that RAGE is a potent inducer of NF-κB signaling and has the unique ability to sustain NF-κB activation through de novo synthesis of *RelA* messenger RNA, providing a constant pool of transcriptional active NF-κB neutralizing endogenous, limiting autoregulatory mechanisms (23).

Downloaded from http://rupress.org/jem/article-pdf/205/2/275/1897784/jem_20070679.pdf by guest on 09 February 2026

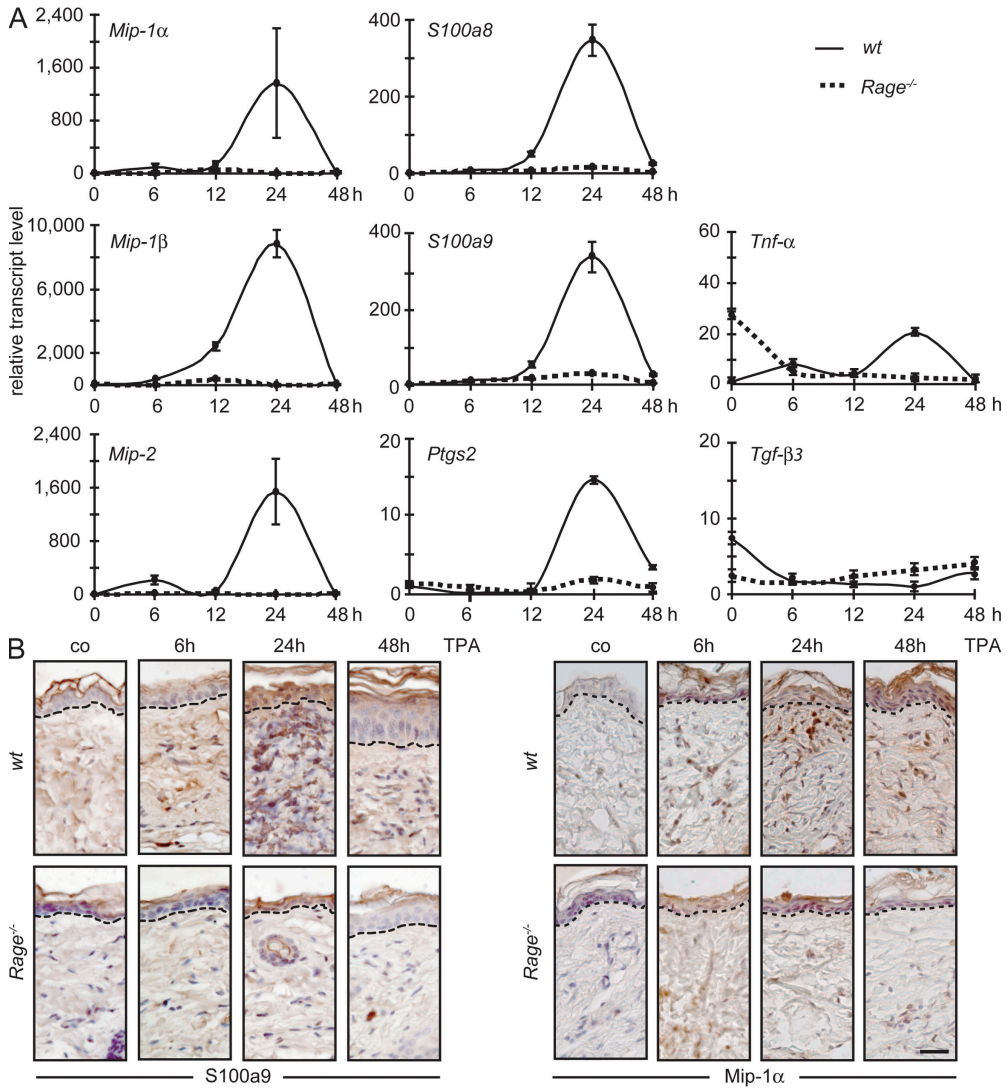

Figure 3. Expression of proinflammatory genes in TPA-treated mice. (A) RQ-PCR was performed with cDNA from total *wt* and *Rage*$^{-/-}$ skin samples treated once with acetone (0 h) or with 10 nmol TPA in acetone and collected at the indicated time points and by using primers for *Mip-1*α, *Mip-1*β, *Mip-2*, *Ptgs2*, *S100a8*, *S100a9*, *Tnf*-α, and *Tgf*-β*3*. Each cDNA from three mice of three separate animal experiments was analyzed in triplicates, and *Hprt* transcripts served as an internal reference. Error bars represent the SEM. (B) Representative pictures of sections derived from tissue specimens as described in A and analyzed for S100a9 and Mip-1α protein expression by IHC staining (brown signal) and followed by counterstaining with hematoxylin. Dashed lines indicate the border between the epidermis and dermis. co, acetone-treated controls. Bar, 20 μm.

Previously, global gene expression profiling on samples from a chemically induced skin carcinogenesis model unraveled strong up-regulation of S100a8 and S100a9 (24), both members of the S100 family of small molecular weight calcium-binding proteins (11). The heterodimeric complex of S100a8/a9 is a well-known extracellular factor that engages with RAGE to induce intracellular signaling (11, 25, 26) and has recently emerged as an important proinflammatory mediator in acute and chronic inflammation (11, 27–29). In line with our previous findings (24), transcription of *S100a8* and *S100a9* was highly elevated in TPA-treated *wt* skin, whereas transcript levels were largely reduced in *Rage*$^{-/-}$ skin (Fig. 3 A). Similar data were obtained in DMBA-initiated and TPA-treated skin, as shown for *S100a8* transcript levels (Fig. S3 C). IHC analysis confirmed differential expression on protein levels (Fig. 3 B and Fig. S5), implying that both act not only as RAGE ligands but also represent target genes of RAGE signaling. This assumption is in accordance with recent findings showing that RAGE maintains cellular activation by induction of its own extracellular ligands (25, 26, 8).

To further strengthen the concept of RAGE-dependent perpetuation of inflammation, we analyzed the consequence of RAGE deficiency on repeated TPA treatment and challenged the back skin three times every 48 h, representing the promotion stage of the DMBA/TPA protocol. *wt* animals developed a strong dermal infiltration and a marked epidermal

Downloaded from http://rupress.org/jem/article-pdf/205/2/275/1897784/jem_20070679.pdf by guest on 09 February 2026

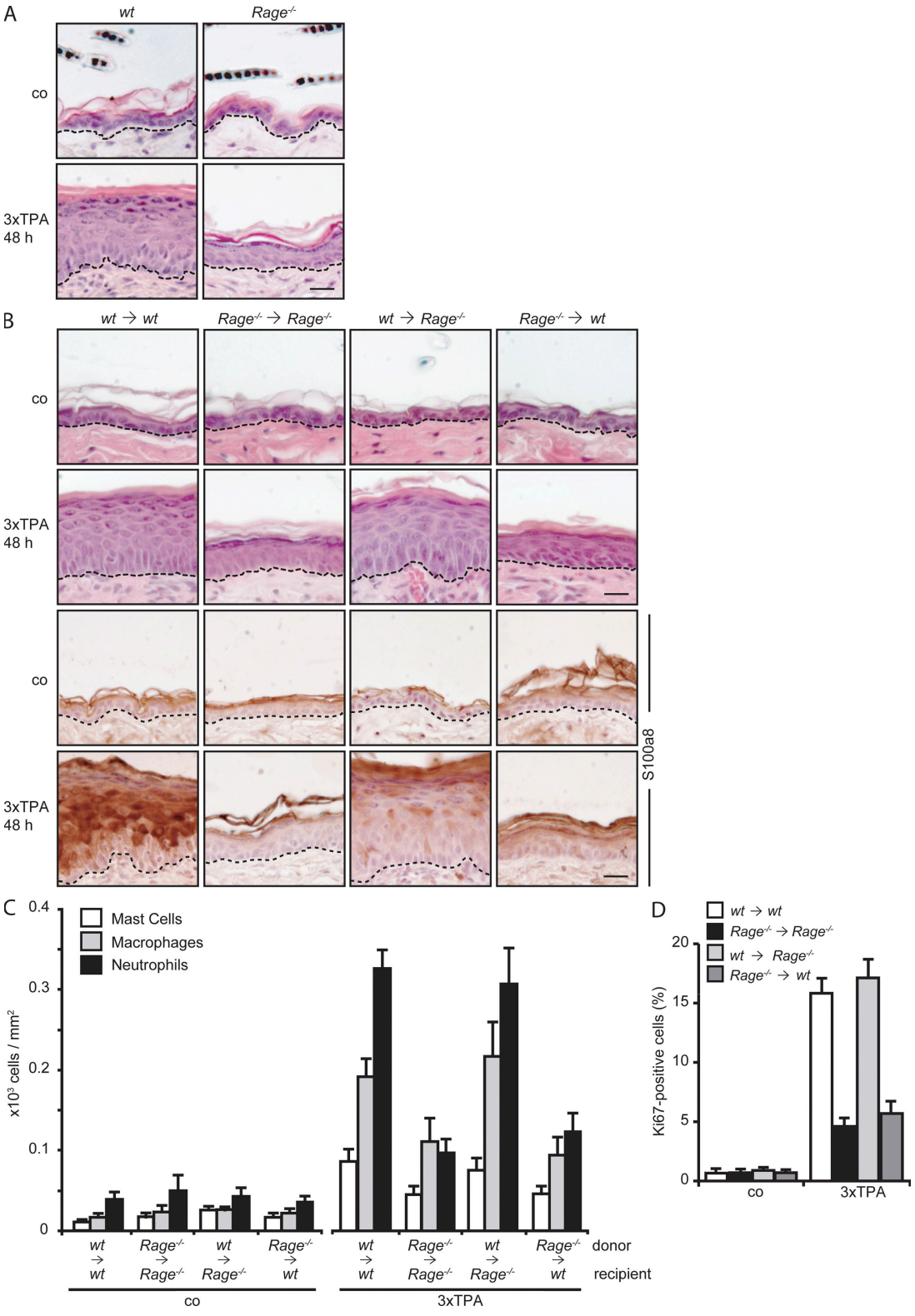

Figure 4. RAGE expression in immune cells is required for TPA-induced dermal infiltration and epidermal hyperplasia. (A) *wt* and *Rage*$^{-/-}$ mice were treated with acetone (co) or 10 nmol of TPA three times every 48 h. Representative images are shown of hematoxylin-eosin–stained skin sections derived from specimens collected 3 d after the final treatment. Dashed lines indicate the border between the epidermis and dermis. Bar, 20 µm. (B) Representative images are shown of hematoxylin-eosin–stained skin sections derived from sublethally irradiated *wt* mice reconstituted with bone marrow

Downloaded from http://rupress.org/jem/article-pdf/205/2/275/1897784/jem_20070679.pdf by guest on 09 February 2026

hyperplasia (Fig. 4 A; and Fig. S6 A, available at http://www.jem.org/cgi/content/full/jem.20070679/DC1). In contrast, *Rage*$^{-/-}$ skin was almost resistant to repeated TPA treatment, with a significant impairment of epidermal hyperplasia (Fig. 4 A), keratinocyte proliferation ($P < 0.003$; Fig. 5 A), dermal infiltration (mast cells, $P < 0.2$; macrophages, $P < 0.0005$; neutrophils, $P < 0.0005$; Fig. S6 A), and up-regulation of S100a8 and S100a9 proteins (Fig. 5 B). Moreover, the number of epidermal keratinocytes with nuclear staining for phosphorylated p65/RelA protein was reduced on tissue sections of *Rage*$^{-/-}$ skin compared with *wt* controls (Fig. S6 B). Collectively, these data suggest that RAGE is essential for TPA-induced tumor promotion, and we indeed found impaired epidermal hyperplasia in DMBA-initiated *Rage*$^{-/-}$ animals upon repeated TPA application after 1 wk as well as after 10 wk in the preneoplastic stage (Fig. S7).

It is noteworthy that S100 and MIP protein expression were detected in both epidermal keratinocytes and a variety of infiltrating immune cells (Fig. S5; and Fig. S8, A and B, available at http://www.jem.org/cgi/content/full/jem.20070679/DC1), implying a critical contribution of multiple cell types in the TPA-induced up-regulation of proinflammatory cytokines. Moreover, RAGE protein is expressed in a variety of distinct cell types (11), including epidermal keratinocytes, tumor cells, endothelial cells, and a subset of innate immune cells such as neutrophils, macrophages, and mast cells (Fig. S8, C and D). To investigate whether RAGE expression on epithelial, endothelial, or immune cells is required for TPA-induced dermal infiltration and epidermal hyperplasia, we analyzed mouse chimera after bone marrow transplantation. As expected, *wt* mice reconstituted with *wt* bone marrow cells (*wt*→*wt*) and *Rage*-deficient mice reconstituted with *Rage*$^{-/-}$ bone marrow cells (*Rage*$^{-/-}$→*Rage*$^{-/-}$) phenocopied the response of *wt* and *Rage*-deficient mice to repeated TPA treatment (Fig. 4, B–D). *Rage*-deficient mice reconstituted with *wt* bone marrow cells (*wt*→*Rage*$^{-/-}$) showed no significant difference in epidermal hyperplasia, keratinocyte proliferation ($P > 0.1$), and dermal infiltration by neutrophils ($P > 0.6$), macrophages ($P > 0.1$), and mast cells ($P > 0.5$) compared with *wt*→*wt* chimera. However, *wt* mice reconstituted with *Rage*$^{-/-}$ bone marrow cells (*Rage*$^{-/-}$→*wt*) revealed impaired epidermal hyperplasia, keratinocyte proliferation ($P < 0.0005$), and dermal infiltration by neutrophils ($P < 0.005$) and macrophages ($P < 0.005$) compared with *Rage*$^{-/-}$→*Rage*$^{-/-}$ chimera. Collectively, we provide experimental evidence that RAGE expression on immune cells, but not keratinocytes or endothelial cells, is required for innate immune cell recruitment and induction of epidermal hyperplasia in vivo, which is in line with published data on a model of HMGB1-induced peritonitis (30). However, IHC analysis on skin sections revealed reduced S100 protein levels for *wt*→*Rage*$^{-/-}$ compared with *wt*→*wt* chimera (Fig. 4 B), demonstrating that RAGE signaling is required for efficient S100a8 and S100a9 expression in keratinocytes.

Based on the bone marrow transfer experiment, the question remained of whether an increase in the amount of infiltrating cells by accelerated TPA application allows complete epidermal hyperplasia and tumor development in *Rage*-deficient mice. Indeed, more frequent TPA application (i.e., three times every 24 h) revealed dermal infiltration, keratinocyte proliferation, and epidermal hyperplasia in *Rage*$^{-/-}$ skin that were almost comparable to *wt* skin (Fig. 5, A and B; and Fig. S6, A and C). Again, expression of S100a8 and S100a9 proteins was only partially restored in keratinocytes of *Rage*$^{-/-}$ skin and did not reach levels that were detected in epidermal keratinocytes of *wt* skin (Fig. 5 B). Finally, we modified the DMBA/TPA protocol by applying TPA every 24 h during the promotion phase, resulting in a complete rescue regarding tumor incidence ($P > 0.2$), with the first tumors appearing in *wt* and *Rage*$^{-/-}$ mice within 5 wk of TPA-induced tumor promotion and with all animals in both groups developing tumors within 6 wk (Fig. 5 C). One explanation for this rescue using an accelerated TPA treatment could be the enhanced expression of other proinflammatory cytokines and activation of bypassing signaling pathways. Indeed, we found high expression of Tnf-α protein in skin and tumor sections of both *wt* and *Rage*$^{-/-}$ mice after TPA application every 24 h (Fig. 5 B; and Fig. S9, available at http://www.jem.org/cgi/content/full/jem.20070679/DC1). However, tumor multiplicity as well as tumor size were only partially restored, because the mean number of tumors per mouse in the group of *Rage*$^{-/-}$ mice reached only 50% of the value determined for the *wt* group, and the tumors of *Rage*$^{-/-}$ mice remained smaller in size compared with *wt* tumors (Fig. 5 C and Fig. S1 B).

In summary, our data provide direct genetic evidence that RAGE mediates sustained skin inflammation upon exposure to the tumor promoter TPA and that RAGE is important for multistage skin carcinogenesis in mice. Given the close association between chronic inflammation and epithelial cancer, we propose that RAGE activation by its ligands, such as S100 proteins, triggers a positive regulatory loop that maintains an inflammatory microenvironment required for the promotion of tumor development. Because other RAGE ligands, such as HMGB1 and AGEs, have been shown to be up-regulated in tumors (8), we cannot exclude that these ligands serve as an additional source of RAGE activation within the established tumor. Although, we found that RAGE expression on immune

cells from *wt* or *Rage*$^{-/-}$ mice (*wt*→*wt* or *Rage*$^{-/-}$→*wt*), or sublethally irradiated *Rage*$^{-/-}$ mice reconstituted with bone marrow cells from wt or *Rage*$^{-/-}$ mice (*wt*→*Rage*$^{-/-}$ or *Rage*$^{-/-}$→*Rage*$^{-/-}$), and were treated as described in A (top two rows). Representative images of sections that were analyzed for S100a8 protein expression by IHC (brown staining; bottom two rows) and that were counterstained with hematoxylin. Dashed lines indicate the border between the epidermis and dermis. Bar, 20 μm. (C) Innate immune cells within the dermis of at least six chimeric mice of each group that were treated as described in B were counted based on specific stainings as described in Fig. 2 C. (D) Percent totals of Ki67-positive keratinocytes of skin specimens from at least three chimera of each group that were treated as described in B, measured, and analyzed as described in Fig. 1 C. Error bars represent the SEM.

Downloaded from http://rupress.org/jem/article-pdf/205/2/275/1897784/jem_20070679.pdf by guest on 09 February 2026

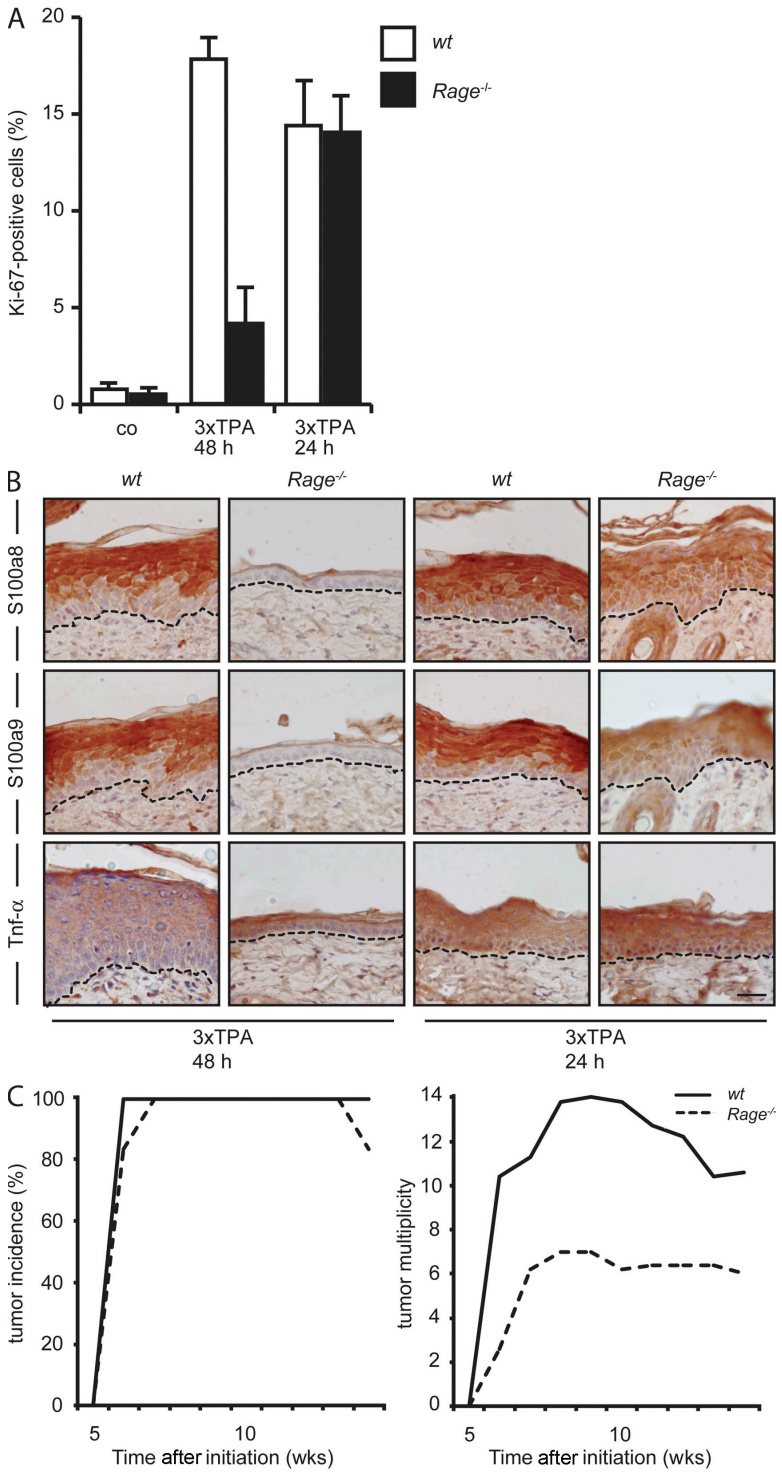

Figure 5. Epidermal hyperplasia and tumor promotion after accelerated TPA treatment. (A) *wt* and *Rage*$^{-/-}$ mice were treated with acetone (co) or 10 nmol TPA three times every 48 or 24 h, respectively, on the shaved back skin. Shown are the percent totals of Ki67-positive keratinocytes of three skin specimens from each genotype that were measured and analyzed as described in Fig. 1 C. (B) Representative images of skin sections from mice treated as described in A that were analyzed for S100a8, S100a9, and Tnf-α protein expression by IHC (brown staining) and counterstained with hematoxylin. Bar, 20 µm. (C) *wt* and *Rage*$^{-/-}$ mice were subjected to a modified DMBA/TPA skin carcinogenesis protocol with TPA treatment every 24 h and were analyzed as described in Materials and methods.

Downloaded from http://rupress.org/jem/article-pdf/205/2/275/1897784/jem_20070679.pdf by guest on 09 February 2026

cells was sufficient for TPA-induced dermal infiltration as well as epidermal hyperplasia, and that accelerated TPA treatment resulted in efficient tumor development in *Rage*$^{-/-}$ animals, we still observed reduced S100a8 and S100a9 protein expression in keratinocytes lacking RAGE expression and only a partial rescue in tumor multiplicity. Thus, RAGE expression on keratinocytes might also contribute to the transformation and malignant progression of epithelial cells, and it will be a challenge for the future to investigate cell type–specific RAGE knockout mice using the DMBA/TPA model. Overall, S100/RAGE signaling appears to be an appropriate target for the development of novel therapies affecting both chronic inflammatory disorders and epithelial malignancies.

MATERIALS AND METHODS

Animals. *Rage*$^{-/-}$ animals were described previously (31, 10), and *wt* controls were obtained from Charles River Laboratories. Both *wt* and *Rage*$^{-/-}$ mice were on a C57BL/6 background (10) and were housed in an insulator under specific pathogen-free and negative-pressure conditions.

Animal work and sample preparation. All animal experiments were performed with 7–9-wk-old female *wt* and *Rage*$^{-/-}$ mice. Skin tumors were generated according to the initiation-promotion protocol of DMBA/TPA-induced multistage carcinogenesis (6), with a single dose of DMBA (100 nmol/100 μl acetone; Sigma-Aldrich) followed by repetitive TPA applications (10 nmol/100 μl acetone) every 48 h (n = 21 mice per genotype) or in an accelerated manner every 24 h (n = 10 mice per genotype). Acetone-treated controls (acetone/acetone, DMBA/acetone, or acetone/TPA) served as internal controls and did not develop any tumors. Tumors were assessed weekly per individuum and were defined as raised lesions of a minimum diameter of 1 mm that had been present for at least two consecutive weeks. Mice were killed 6 wk after the final treatment (representing week 36 after initiation for the classical protocol and week 13 after initiation for the accelerated protocol). For single and repetitive TPA application, *wt* and *Rage*$^{-/-}$ animals were shaved on the dorsal skin and treated 3 d later topically with 100 μl acetone as a control or TPA (10 nmol/100 μl acetone; n = 6 mice per genotype and treatment). Chronic responses were achieved by 3× topical treatment every 48 h or every 24 h, respectively (n = 6 mice per genotype and treatment). Animals were killed at the times indicated in the figures or 3 d after the final application. Initiation was achieved with a single treatment with DMBA (100 nmol/100 μl acetone) or with 100 μl acetone as a control 1 wk before topical TPA treatment (n = 4 mice per genotype and treatment). Tumors and skin necropsies were immediately frozen in liquid nitrogen after isolation for RNA preparation. For histological analysis, tissues were fixed with 4% paraformaldehyde (PFA) in PBS, pH 7.4, paraffin embedded, or embedded in optimum cutting temperature cryomedium (Sakura) and, subsequently, cut into 6-μm sections as described previously (24, 32). Tissue sections were stained with hematoxylin-eosin and were examined by several experienced experimenters. The procedures for performing animal experiments were in accordance with the principles and guidelines of the Arbeitsgemeinschaft der Tierschutzbeauftragten in Baden-Württemberg and were approved by the Regierungspräsidium of Karlsruhe, Germany (AZ 129/02).

Generation of bone marrow chimeras. Bone marrow chimeras were prepared as described previously (33). Reconstitution was confirmed by FACS analysis using specific markers for leukocyte populations (unpublished data). TPA treatment was performed 10 wk after the bone marrow transfer.

Tumor grading. Hematoxylin-eosin–stained tissue sections of *wt* and *Rage*$^{-/-}$ tumors were graded in a blinded manner by two experts in mouse skin pathology. Grades followed a recent publication (34) and were assigned as follows: papilloma grade 1, papilloma grade 2, papilloma with focal microinvasion, or squamous cell carcinoma.

BrdU incorporation assay. BrdU in vivo incorporation was performed according to the manufacturer's recommendations (Roche). Mice were injected into the tail vein with 100 μg/g BrdU dissolved in PBS 90 min before sacrifice. The skin was fixed with 4% PFA in PBS, pH 7.4, and paraffin embedded. Tissue sections were analyzed by IF stainings.

Histochemical and immunostaining analyses. IHC analysis on paraffin sections was performed according to the manufacturer's instructions (Vector Laboratories), and sections were counterstained with hematoxylin. IF analysis was performed as described previously (19, 32, 35), and nuclear staining was done with H33342 (EMD). A summary of all primary antibodies that were used is provided in Table S1 (available at http://www.jem.org/cgi/content/full/jem.20070679/DC1). For BrdU detection, IF analysis was performed using the M.O.M. immunodetection kit (Vector Laboratories). Mast cells on tissue sections were detected by toluidine blue staining. TUNEL assay was performed using the In Situ Cell Death Detection Kit, according to the manufacturer's recommendations (Roche).

Image analysis. Tissue sections derived from at least three independent samples per genotype were analyzed by experimenters without the knowledge of the coded sample identity. Stained sections were visualized by bright field or IF microscopy (DMLB; Leica) using a digital camera (DXM1200; Nikon) and software (ACT-1; Nikon). Confocal microscopy was done using a confocal microscope (TCS SP5; Leica) and software (LAS AF; Leica). Image processing was performed with Photoshop CS software (Adobe).

RQ-PCR. Total RNA was isolated from mouse back skin necropsies using peqGOLD RNAPure (peqlab Biotechnologie) according to the manufacturer's protocol. RNA integrity was confirmed by agarose gel electrophoresis (Agilent Bioanalyzer 2100; Agilent Technologies). RNA was reverse transcribed using RevertAid H Minus-MuLV RT (Fermentas) and oligo-dT primers, followed by standard RQ-PCR performed on a detection system (MyiQ; Bio-Rad Laboratories) using the Absolute QPCR SYBR green fluorescein mix (Abgene). Primer sequences are listed in Table S2 (available at http://www.jem.org/cgi/content/full/jem.20070679/DC1). Target gene computed tomography (CT) values were normalized to the corresponding CT values of *Hprt* using the ΔCT method. Expression levels for acetone-treated *wt* controls were set to one to calculate relative transcript levels. Each cDNA was analyzed in triplicates, and the error bars represent the SEM.

Statistical analysis. For the statistical analysis of the DMBA/TPA experiments, the exact Wilcoxon rank sum test was used for comparison of the individual maximum number of papilloma of each animal, and the log-rank test was used for the comparison of the time to first papilloma (6). The proliferation index was calculated from the percentage of total of BrdU- or Ki67-positive epithelial cells, which were counted on stained skin or tumor sections from at least three different samples of each genotype. Quantification of innate immune cells was performed with stained skin or tumor sections of *wt* and *Rage*$^{-/-}$ mice. Stained cells were counted on tissue sections from three different papillomas of each genotype or from three different mice of each genotype per treatment and/or time point. As multiple measurements were obtained from every tumor or skin sample, mixed linear models were used to test whether the variables of interest differ between the genotypes. The analyses were performed using PROC MIXED (version 9.1; SAS Institute, Inc.) with compound symmetry covariance structure. QQ plots were used to assess whether the variables of interest follow a normal distribution. However, nonparametric alternatives are not available for the analysis of repeated measures. The columns represent means and the error bars represent the SEM for the mean values. $P \leq 0.05$ was considered significant. In all cases, the group size was chosen to produce results that are statistically unambiguous.

Online supplemental material. Table S1 lists all antibodies used for IHC and IF analysis, and Table S2 lists all sequences of primers used for RQ-PCR. Fig. S1 provides tumor sizes and grading of the chemically induced skin tumors derived from *wt* and *Rage*$^{-/-}$ mice. Fig. S2 shows quantifications of

Downloaded from http://rupress.org/jem/article-pdf/205/2/275/1897784/jem_20070679.pdf by guest on 09 February 2026

BrdU- and phospho–c-Jun–positive tumor cells on *wt* and *Rage*$^{-/-}$ skin tumors. It further shows representative images of *wt* and *Rage*$^{-/-}$ tumor sections stained for infiltrating immune cells. Fig. S3 gives data on DMBA-initiated and single TPA-treated *wt* and *Rage*$^{-/-}$ mice, including histological skin sections, quantifications of infiltrating immune cells within the dermis, and *S100a8* transcript levels. Fig. S4 provides representative images of *wt* and *Rage*$^{-/-}$ tumor sections that were stained for COX-2, Mip-1α, Mip-1β, and Mip-2 proteins. Fig. S5 shows IHC stainings for S100a8, Mip-1β, and Mip-2 proteins on single TPA-treated *wt* and *Rage*$^{-/-}$ skin sections. Fig. S6 provides quantification of infiltrating immune cells within the dermis of *wt* and *Rage*$^{-/-}$ mice treated three times with TPA every 48 or 24 h, respectively. It further provides representative images of histological sections from 3× TPA-treated *wt* and *Rage*$^{-/-}$ skin specimens and sections stained for phospho-p65 protein. Fig. S7 gives data on DMBA-initiated and repeatedly TPA-treated (for 1 and 10 wk, respectively) *wt* and *Rage*$^{-/-}$ mice, including histological skin sections. Fig. S8 provides representative images of tumor sections from *wt* and *Rage*$^{-/-}$ skin tumors costained for S100a8, RAGE, neutrophils, macrophages, mast cells, and endothelial cells using confocal microscopy. Fig. S9 provides representative images of tumor sections derived from *wt* and *Rage*$^{-/-}$ that were treated according to the classical and the accelerated carcinogenesis protocol and were stained for Tnf-α protein. Online supplemental material is available at http://www.jem.org/cgi/content/full/jem.20070679/DC1.

We thank A. Erhardt, A. Krischke, S. Paljevic, A. Strecker, I. Vogt, and K. Zipp for excellent technical assistance, and we are very grateful to A. Kopp-Schneider for the statistical analysis and to J. Beaudouin for help with confocal imaging.

This work was supported in part by the German Ministry for Education and Research (National Genome Research Network grant NGFN-2, 01GS0460/01GR0418 to P. Angel), the Research Training Network (grant HPRN-CT2002-00256 to P. Angel), the DKFZ-MOST German-Israeli Cooperation Program in Cancer Research (grant Ca-117 to P. Angel), the German Society of Dermatology (grant DDG/D.10050498/Di to C. Gebhardt), and the Deutsche Forschungsgemeinschaft (grant DFG/SFB 405 to P.P. Nawroth). C. Gebhardt holds a Young Investigator Award of the Faculty of Medicine at the University of Heidelberg. M. Durchdewald is supported by the Studienstiftung des deutschen Volkes.

The authors have no conflicting financial interests.

Submitted: 4 April 2007
Accepted: 7 December 2007

REFERENCES

1. Hanahan, D., and R.A. Weinberg. 2000. The hallmarks of cancer. *Cell*. 100:57–70.
2. DiGiovanni, J. 1992. Multistage carcinogenesis in mouse skin. *Pharmacol. Ther.* 54:63–128.
3. Coussens, L.M., and Z. Werb. 2002. Inflammation and cancer. *Nature*. 420:860–867.
4. Balkwill, F., K.A. Charles, and A. Mantovani. 2005. Smoldering and polarized inflammation in the initiation and promotion of malignant disease. *Cancer Cell*. 7:211–217.
5. de Visser, K.E., A. Eichten, and L.M. Coussens. 2006. Paradoxical roles of the immune system during cancer development. *Nat. Rev. Cancer*. 6:24–37.
6. Furstenberger, G., and A. Kopp-Schneider. 1995. Malignant progression of papillomas induced by the initiation-promotion protocol in NMRI mouse skin. *Carcinogenesis*. 16:61–69.
7. Moore, R.J., D.M. Owens, G. Stamp, C. Arnott, F. Burke, N. East, H. Holdsworth, L. Turner, B. Rollins, M. Pasparakis, et al. 1999. Mice deficient in tumor necrosis factor-alpha are resistant to skin carcinogenesis. *Nat. Med.* 5:828–831.
8. Schmidt, A.M., S.D. Yan, S.F. Yan, and D.M. Stern. 2001. The multiligand receptor RAGE as a progression factor amplifying immune and inflammatory responses. *J. Clin. Invest.* 108:949–955.
9. Bierhaus, A., P.M. Humpert, M. Morcos, T. Wendt, T. Chavakis, B. Arnold, D.M. Stern, and P.P. Nawroth. 2005. Understanding RAGE, the receptor for advanced glycation end products. *J. Mol. Med.* 83:876–886.
10. Liliensiek, B., M.A. Weigand, A. Bierhaus, W. Nicklas, M. Kasper, S. Hofer, J. Plachky, H.J. Grone, F.C. Kurschus, A.M. Schmidt, et al. 2004. Receptor for advanced glycation end products (RAGE) regulates sepsis but not the adaptive immune response. *J. Clin. Invest.* 113:1641–1650.
11. Gebhardt, C., J. Nemeth, P. Angel, and J. Hess. 2006. S100A8 and S100A9 in inflammation and cancer. *Biochem. Pharmacol.* 72:1622–1631.
12. Eferl, R., and E.F. Wagner. 2003. AP-1: a double-edged sword in tumorigenesis. *Nat. Rev. Cancer*. 3:859–868.
13. Hsu, T.C., M.R. Young, J. Cmarik, and N.H. Colburn. 2000. Activator protein 1 (AP-1)- and nuclear factor kappaB (NF-kappaB)-dependent transcriptional events in carcinogenesis. *Free Radic. Biol. Med.* 28:1338–1348.
14. Karin, M., and F.R. Greten. 2005. NF-kappaB: linking inflammation and immunity to cancer development and progression. *Nat. Rev. Immunol.* 5:749–759.
15. Taguchi, A., D.C. Blood, G. del Toro, A. Canet, D.C. Lee, W. Qu, N. Tanji, Y. Lu, E. Lalla, C. Fu, et al. 2000. Blockade of RAGE-amphoterin signalling suppresses tumour growth and metastases. *Nature*. 405:354–360.
16. Tiano, H.F., C.D. Loftin, J. Akunda, C.A. Lee, J. Spalding, A. Sessoms, D.B. Dunson, E.G. Rogan, S.G. Morham, R.C. Smart, and R. Langenbach. 2002. Deficiency of either cyclooxygenase (COX)-1 or COX-2 alters epidermal differentiation and reduces mouse skin tumorigenesis. *Cancer Res.* 62:3395–3401.
17. Shanmugam, N., Y.S. Kim, L. Lanting, and R. Natarajan. 2003. Regulation of cyclooxygenase-2 expression in monocytes by ligation of the receptor for advanced glycation end products. *J. Biol. Chem.* 278:34834–34844.
18. Bianchi, R., C. Adami, I. Giambanco, and R. Donato. 2007. S100B binding to RAGE in microglia stimulates COX-2 expression. *J. Leukoc. Biol.* 81:108–118.
19. Muller-Decker, K., G. Neufang, I. Berger, M. Neumann, F. Marks, and G. Furstenberger. 2002. Transgenic cyclooxygenase-2 overexpression sensitizes mouse skin for carcinogenesis. *Proc. Natl. Acad. Sci. USA*. 99:12483–12488.
20. Jamieson, T., D.N. Cook, R.J. Nibbs, A. Rot, C. Nixon, P. McLean, A. Alcami, S.A. Lira, M. Wiekowski, and G.J. Graham. 2005. The chemokine receptor D6 limits the inflammatory response in vivo. *Nat. Immunol.* 6:403–411.
21. Nibbs, R.J., D.S. Gilchrist, V. King, A. Ferra, S. Forrow, K.D. Hunter, and G.J. Graham. 2007. The atypical chemokine receptor D6 suppresses the development of chemically induced skin tumors. *J. Clin. Invest.* 117:1884–1892.
22. Pikarsky, E., and Y. Ben-Neriah. 2006. NF-kappaB inhibition: a double-edged sword in cancer? *Eur. J. Cancer*. 42:779–784.
23. Bierhaus, A., S. Schiekofer, M. Schwaninger, M. Andrassy, P.M. Humpert, J. Chen, M. Hong, T. Luther, T. Henle, I. Kloting, et al. 2001. Diabetes-associated sustained activation of the transcription factor nuclear factor-kappaB. *Diabetes*. 50:2792–2808.
24. Gebhardt, C., U. Breitenbach, J.P. Tuckermann, B.T. Dittrich, K.H. Richter, and P. Angel. 2002. Calgranulins S100A8 and S100A9 are negatively regulated by glucocorticoids in a c-Fos-dependent manner and overexpressed throughout skin carcinogenesis. *Oncogene*. 21:4266–4276.
25. Hofmann, M.A., S. Drury, C. Fu, W. Qu, A. Taguchi, Y. Lu, C. Avila, N. Kambham, A. Bierhaus, P. Nawroth, et al. 1999. RAGE mediates a novel proinflammatory axis: a central cell surface receptor for S100/calgranulin polypeptides. *Cell*. 97:889–901.
26. Andrassy, M., J. Igwe, F. Autschbach, C. Volz, A. Remppis, M.F. Neurath, E. Schleicher, P.M. Humpert, T. Wendt, B. Liliensiek, et al. 2006. Posttranslationally modified proteins as mediators of sustained intestinal inflammation. *Am. J. Pathol.* 169:1223–1237.
27. Zenz, R., R. Eferl, L. Kenner, L. Florin, L. Hummerich, D. Mehic, H. Scheuch, P. Angel, E. Tschachler, and E.F. Wagner. 2005. Psoriasis-like skin disease and arthritis caused by inducible epidermal deletion of Jun proteins. *Nature*. 437:369–375.
28. Hiratsuka, S., A. Watanabe, H. Aburatani, and Y. Maru. 2006. Tumour-mediated upregulation of chemoattractants and recruitment of myeloid cells predetermines lung metastasis. *Nat. Cell Biol.* 8:1369–1375.
29. Vogl, T., K. Tenbrock, S. Ludwig, N. Leukert, C. Ehrhardt, M.A. van Zoelen, W. Nacken, D. Foell, T. van der Poll, C. Sorg, and J. Roth.

Downloaded from http://rupress.org/jem/article-pdf/205/2/275/1897784/jem_20070679.pdf by guest on 09 February 2026

2007. Mrp8 and Mrp14 are endogenous activators of Toll-like receptor 4, promoting lethal, endotoxin-induced shock. *Nat. Med.* 13:1042–1049.
30. Orlova, V.V., E.Y. Choi, C. Xie, E. Chavakis, A. Bierhaus, E. Ihanus, C.M. Ballantyne, C.G. Gahmberg, M.E. Bianchi, P.P. Nawroth, and T. Chavakis. 2007. A novel pathway of HMGB1-mediated inflammatory cell recruitment that requires Mac-1-integrin. *EMBO J.* 26:1129–1139.
31. Constien, R., A. Forde, B. Liliensiek, H.J. Grone, P. Nawroth, G. Hammerling, and B. Arnold. 2001. Characterization of a novel EGFP reporter mouse to monitor Cre recombination as demonstrated by a Tie2 Cre mouse line. *Genesis.* 30:36–44.
32. Muller-Decker, K., G. Furstenberger, N. Annan, D. Kucher, A. Pohl-Arnold, B. Steinbauer, I. Esposito, S. Chiblak, H. Friess, P. Schirmacher, and I. Berger. 2006. Preinvasive duct-derived neoplasms in pancreas of keratin 5-promoter cyclooxygenase-2 transgenic mice. *Gastroenterology.* 130:2165–2178.
33. Lumsden, J.M., J.A. Williams, and R.J. Hodes. 2003. Differential requirements for expression of CD80/86 and CD40 on B cells for T-dependent antibody responses in vivo. *J. Immunol.* 170:781–787.
34. Thomas-Ahner, J.M., B.C. Wulff, K.L. Tober, D.F. Kusewitt, J.A. Riggenbach, and T.M. Oberyszyn. 2007. Gender differences in UVB-induced skin carcinogenesis, inflammation, and DNA damage. *Cancer Res.* 67:3468–3474.
35. Gebhardt, C., U. Breitenbach, K.H. Richter, G. Furstenberger, C. Mauch, P. Angel, and J. Hess. 2005. c-Fos-dependent induction of the small ras-related GTPase Rab11a in skin carcinogenesis. *Am. J. Pathol.* 167:243–253.

Downloaded from http://rupress.org/jem/article-pdf/205/2/275/1897784/jem_20070679.pdf by guest on 09 February 2026